Journal of Neuroradiology 46 (2019) 214–221

Available online at ScienceDirect www.sciencedirect.com

Elsevier Masson France EM|consulte www.em-consulte.com

Original Article

Susceptibility weighted imaging in infants with staged embolization of vein of Galen aneurysmal malformations

Amgad El Mekabaty [a], Monica S. Pearl [a], Bommy Mershon [b], Ivor Berkowitz [b], Philippe Gailloud [a], Thierry A.G.M. Huisman [c,*]

[a] Division of Interventional Neuroradiology, Russell H. Morgan Department of Radiology and Radiological Science, Johns-Hopkins University School of Medicine, Baltimore, Maryland, USA
[b] Department of Anesthesiology and Critical Care, Johns Hopkins University School of Medicine, Baltimore, Maryland, USA
[c] Division of Pediatric Radiology and Pediatric Neuroradiology, Russell H. Morgan Department of Radiology and Radiological Science, Johns-Hopkins University School of Medicine, Baltimore, Maryland, USA

ARTICLE INFO

Article history:
Available online 10 November 2018

Keywords:
Vein of galen aneurysmal malformation
Embolization
Susceptibility weighted imaging
Children

ABSTRACT

Background and purpose. – The vein of Galen aneurysmal malformation (VGAM) is a rare congenital vascular malformation with a higher morbidity and mortality, especially in neonates. Ultrasound, CT and MR are usually used in diagnosis and treatment monitoring of these disorders. In this current study, we aim to examine utility of SWI in evaluation of treatment response in infants with VGAM.
Materials and methods. – We performed a retrospective chart analysis of children with VGAM in our institution between January 2008 and December 2016. Inclusion criteria included; confirmed VGAM on DSA; available SWI sequence at baseline and at follow up after at least a single embolization session; age at initial MR of 18 years or younger. Signal intensity and Angioarchitecture of VGAM and cerebral veins on SWI, as well as hydrocephalus and clinical outcome were evaluated.
Results. – Of 11 patients identified with VGAM in our institution, 5 children (3 males and 2 females) satisfied the inclusion criteria. The average age at initial MR was 29 days (range 1–120). Fourteen MRI were available for review. All children had VGAM of mural type. Intramedullary veins were dilated and SWI-hypointense in all children, while subependymal and sulcal veins were dilated and SWI-hypointense in 4 patients on initial MRI. On the first available follow up MRI, cerebral veins have mostly normalized in 4 children and remained mostly dilated and SWI-hypointense in 1 child; even after complete treatment of the VGAM.
Conclusion. – Our preliminary findings show that SWI seems to offer a beneficial non-invasive tool in evaluating passive venous congestion patterns in pediatric patients with VGAM. It remains to be determined in larger studies, the clinical significance of these SWI changes.

Background and purpose

The vein of Galen aneurysmal malformation (VGAM) is a rare congenital vascular malformation representing 1% of all pediatric congenital anomalies, yet it comprises up to 30% of pediatric vascular congenital anomalies [1,2]. These malformations are characterized by arteriovenous fistulae draining into the persistent and dilated fetal median prosencephalic vein of Markowski [3], which is the embryonic precursor of vein of Galen in adults [4]. They are considered to form between the 6th and 11th weeks of gestation when such a fetal venous draining system exists [5]. VGAM is associated with a high morbidity and mortality, especially in the neonatal period [6–8]. The current most accepted modality of treatment for VGAM is a staged endovascular embolization of the arterial feeders with or without embolization of the venous sac [1,7,9–11]. Goal is to reduce the high-flow arteriovenous shunting and resultant cardiac failure, while reducing the likelihood of adverse events such as normal perfusion pressure breakthrough phenomenon [10,12]. The diagnosis and monitoring is usually performed with transfontanellar ultrasound (US) and computed tomography (CT) or magnetic resonance imaging/angiography (MRI/MRA). These methods suffer from several limitations, such as operator dependency, reduced accuracy of US [13], and the carcinogenic risk associated with ionizing radiation (CT) [14]. Pre- and post-natal conventional T1

* Corresponding author at: Russell H. Morgan Department of Radiology and Radiological Science, The Johns-Hopkins Hospital, 1800, Orleans street, Zayed 4174, 21287 Baltimore, MD USA.
E-mail address: thuisma1@jhmi.edu (T.A.G.M. Huisman).

https://doi.org/10.1016/j.neurad.2018.09.009
0150-9861/

and T2-weighted MRI and Time-of-Flight or Phase Contrast MRA have proven to be a valuable alternative imaging modality for the diagnostic work up of these complex malformations. These techniques, however, are limited for the evaluation of the intracerebral venous hypertension that is typically characterized by dilated intramedullary veins. A new, advanced MRI sequence known as susceptibility-weighted imaging (SWI), which has a high intrinsic sensitivity for venous blood has proven its value for various pediatric neurological disease [15,16], especially for vascular disorders such as VGAM [17]. SWI is a high-spatial resolution, gradient echo MRI-sequence, which accentuates the magnetic susceptibility differences between de-oxygenated blood in the veins compared to the adjacent oxygenated tissues [18]. In this blood oxygen level dependent (BOLD) venography principle of SWI, the normal draining veins show a hypointense signal owing to the de-oxygenated hemoglobin, while arterialized veins (e.g. with dural arteriovenous fistula "DAVF" or VGAM) appear SWI-hyperintense due to arteriovenous shunting [17,19,20]. SWI has also proven helpful in differentiating between dilated pial veins from arteriovenous shunting and passive venous congestion in DAVF in adults [21,22]. Jagadeesan et al. [17], showed in their series that SWI was even helpful in accurately discriminating between high-flow and low-flow abnormalities of vein of Galen. The role of the SWI technique in evaluating staged treatment of VGAM has not been previously described. The aim of our study is to examine the utility of the SWI technique as a non-invasive method for evaluating treatment response, assessing the degree of arteriovenous shunting and passive venous congestion after endovascular embolization of VGAM.

Materials and methods

Patient population and clinical features

We performed an electronic search of our prospectively maintained and institutional review board (IRB)-approved pediatric neuroradiology database between January 2008 and December 2016, for patients with "true" VGAM (i.e. pediatric patients with pial arteriovenous malformation draining into a dilated vein of Galen "VGAD" were not included). Inclusion criteria included the following:

- confirmed diagnosis of VGAM on DSA;
- availability of MR imaging study of adequate diagnostic quality, including a SWI sequence, at the time of diagnosis before any endovascular intervention;
- performance of at least one session of endovascular embolization;
- availability of a follow-up MR imaging study including SWI after at least one endovascular embolization session and;
- age at initial MR imaging of 18 years or younger.

Children with MR studies without an SWI sequence were excluded from the study. Patient's demographics, clinical presentation, blood oxygenation level during the MRI, anesthetic agent if MRI was performed under general anesthesia (GA), time between MRI and endovascular embolization, number of staged endovascular embolization sessions, degree of arteriovenous (AV) shunting reduction after each session and major peri-procedural complications related to endovascular embolization, were collected.

Image acquisition

The SWI sequence dataset contained 4 types of images:

- original magnitude image;
- phase mask image;
- combined SWI processed magnitude image, which is obtained through multiplying the original magnitude and phase mask images; and;
- minimum intensity projection (minIP) image of the combined SWI processed magnitude image.

The minIP images were produced using contiguous sections with thickness of 8 mm (8 contiguous 1 mm slices in infants) or 16 mm (8 contiguous 2 mm slices in children > 2 years), in order to avoid average volume artifact and any subsequent misregistration of vessels. All imaging, conventional and SWI were obtained on a 3.0 T MRI scanner (Skyra, Siemens, Erlangen, Germany). The imaging parameters for the SWI sequence were as follows: TR 49 ms, TE 40 ms, flip angle 15°, bandwidth 80 kHz, slice thickness 2.0 mm, FOV 201 × 230 mm, matrix size 320 × 221 and integrated parallel acquisition technique factor of 2. The SWI acquisition time is 4.57 min.

Image analysis

For the purpose of this study, in addition to the evaluation of the angioarchitecture of the VGAM and degree of white matter edema, the conventional T1 and T2-weighted MR images were specifically evaluated for the degree of ventriculomegaly and width of the subarachnoid spaces. The ventricles and subarachnoid spaces were graded as normal, versus mildly, moderately or severely enlarged. The following venous structures were reviewed on the SWI images:

- vein of Galen;
- subependymal veins;
- intramedullary veins; and;
- sulcal veins.

For each location, the appearance of the veins on SWI was classified as:

- non-visible;
- visible, or;
- visible and dilated.

The signal intensity of the veins as seen on minIP SWI were graded as hypointense, isointense or hyperintense compared to the adjacent brain parenchyma. For patients in whom an endovascular embolization of the vein of Galen was performed, the SWI signal intensity of the vein of Galen was noted as "coil mass" on follow-up MR imaging. The coils within the vein of Galen prevent adequate evaluation of the intravascular signal intensity due to the coil related susceptibility artifacts with subsequent SWI-hypointensity/signal void. All images were evaluated by a dedicated pediatric neuroradiologist with more than 2 decades of experience (TAGMH).

Catheter angiography was performed in all patients in a biplane neuroangiography suite (Axiom Artis Zee, Siemens, Erlangen, Germany) using dedicated pediatric DSA protocols. Two experienced interventional neuroradiologists (MP and PG) reviewed the initial conventional angiography images to verify the presence of VGAM and characterize the angioarchitectural features (i.e. mural, choroidal or combined type [12]). The follow-up DSAs after each staged endovascular embolization treatment session were also evaluated and the reduction in degree of AV shunting was graded as: mild (< 33%), moderate (34–66%), significant reduction (67%–99%) or complete occlusion of VGAM (100%). Endovascular embolization was performed utilizing a combination of coils and n-butyl cyanoacrylate (nBCA) for the arterial feeders and coils for the venous sac of the VGAM. Pearson's correlation coefficient (r) was

Table 1
Patient characteristics and clinical presentation.

No.	Age at 1st MRI (days)	Gender	Diagnosis	Clinical presentation	No. of SWI studies	No. of staged embolization sessions
1	120	F	VGAM* (mural type)	Diagnosed prenatally mild right ventricular hypertrophy cardiac arrhythmia with WPW*	2	1
2	7	M	VGAM* (mural type)	Cardiomegaly persistent pulmonary hypertension of neonate	3	3
3	1	M	VGAM* (mural type)	Polyhydramnios and fetal hydrops cardiomegaly with poor function hepatomegaly	2	3
4	11	F	VGAM* (mural type)	Congestive heart failure hypertension respiratory failure	4	5
5	6	M	VGAM* (mural type)	Diagnosed prenatally heart failure macrocephaly and seizures	3	2

* VGAM; Vein of Galen aneurysmal malformation, WPW; Wolff-Parkinson-White syndrome.

Table 2
Oxygen saturation (SaO2, %) and anesthetic agents used during MRI.

No.	Pre-procedural MRI		1st FU MRI		2nd FU MRI		3rd FU MRI	
	SaO_2	Anesthetic agent	SaO_2	Anesthetic agent	SaO_2	Anesthetic agent	SaO_2	Anesthetic agent
1	100	Isoflurane	100	Isoflurane	–	–	–	–
2	> 95	N/S	100	Isoflurane	99	Isoflurane	–	–
3	> 95	N/S	100	Isoflurane	–	–	–	–
4	> 95	N/S	99	Isoflurane	93	Sevoflurane	100	Isoflurane
5	N/A	N/A	100	Isoflurane	100	Isoflurane	–	–

N/S: natural sleep; N/A: not available (outside study).

calculated for correlation of normalization of appearance of cerebral veins on SWI (dichotomized as either mostly or completely normalized vs. no normalization) with degree of arteriovenous shunting reduction after embolization, hydrocephalus, postprocedural complications and clinical outcome.

Results

Between January 2008 and December 2016, 11 pediatric patients with VGAM underwent endovascular treatment in our institution. Of these 11 patients, 5 children (3 males and 2 females) fulfilled all inclusion criteria and were included in this study. There were 14 MRI studies (range 2–4 MRI studies per patient) available for evaluation. The average age at the first MRI study was 29 days (range 1–120 days). The number of endovascular embolization sessions ranged between 1–7 sessions. Patient characteristics and clinical presentation are listed in Table 1. All patients were found to have VGAM of the mural type on DSA. Ten (71%) MRI studies were performed under GA with an average oxygen saturation (SaO2) of 99.1% (range 93–100%), 3 (21%) MR studies were performed in natural sleep with an average SaO2 greater than 95%, while anesthesia information was not available in one (8%) study. Detailed SaO2 data and relevant anesthesia information are listed in Table 2.

Findings on baseline MRI study

On the initial MRI, 2 patients had moderate ventriculomegaly, 1 patient had mild ventriculomegaly, and 2 had a normal sized ventricular system. The subarachnoid spaces were mildly widened in 4 patients and normal in one patient. The vein of Galen was SWI-hyperintense on the initial MR studies in all children. The subependymal and sulcal veins were SWI-hypointense, visible and dilated 4 patients and non-visible in 1 (Case 1; online supplementary Fig. 1). The intramedullary veins were SWI-hypointense, visible and dilated in all patients. In one patient (Case 4) there was evidence of a chronic occlusion of the posterior third of the superior sagittal sinus (SSS) on SWI and time of flight (TOF) MR venography (MRV). The average time interval from initial MRI study to the first embolization session was 29 days (range 0–121). Prior to the first available follow-up MRI with SWI sequence, case 1, 2 and 5 received one embolization session, case 3 received 2 embolization sessions and case 4 received 4 embolization sessions resulting in a significant reduction of the AV shunting in 2 children and a mild reduction in the remaining 3 children.

Findings on first follow-up MRI

The average time interval between the most recent embolization session to the first follow-up MRI study was 86 days (range 0–256). On the first follow-up MR study, 2 children had severe ventriculomegaly; 2 moderate ventriculomegaly; and 1 had a normal sized ventricular system. The subarachnoid spaces were mildly widened in 3 children, moderately widened in one child and not widened in one patient. The dilatation of the vein of Galen normalized in one child (Case 1). In 2 children (Cases 2 and 5) the vein of Galen remained dilated and SWI-hyperintense. The remaining 2 children had a “coil mass” in the vein of Galen precluding evaluation of the SWI-signal intensity. Subependymal and intramedullary veins were non-visible on SWI in 4 patients, and remained SWI-hypointense, visible and dilated in 1 patient (Case 5). Sulcal veins were non-visible on SWI in 3 patients, and remained SWI-hypointense, visible and dilated in 2 children (Case 2 and 5).

Three children received additional staged embolization (Cases 2, 4 and 5). The average time from first follow-up MR study to the second embolization session was 7 days (range 0–20). Complete reduction in AV shunting was achieved in 2 children (Case 2 and 5) and mild reduction was achieved in one child (Case 4).

Findings on further follow-up SWI

The average time from the second embolization session to second follow-up MRI study was 39 days (range 19–60). On the second follow-up MR study, 2 children had severe ventriculomegaly and 1 child had mild ventriculomegaly. The vein of Galen remained SWI-hyperintense in 1 child (Case 2; online supplementary Fig. 2). The

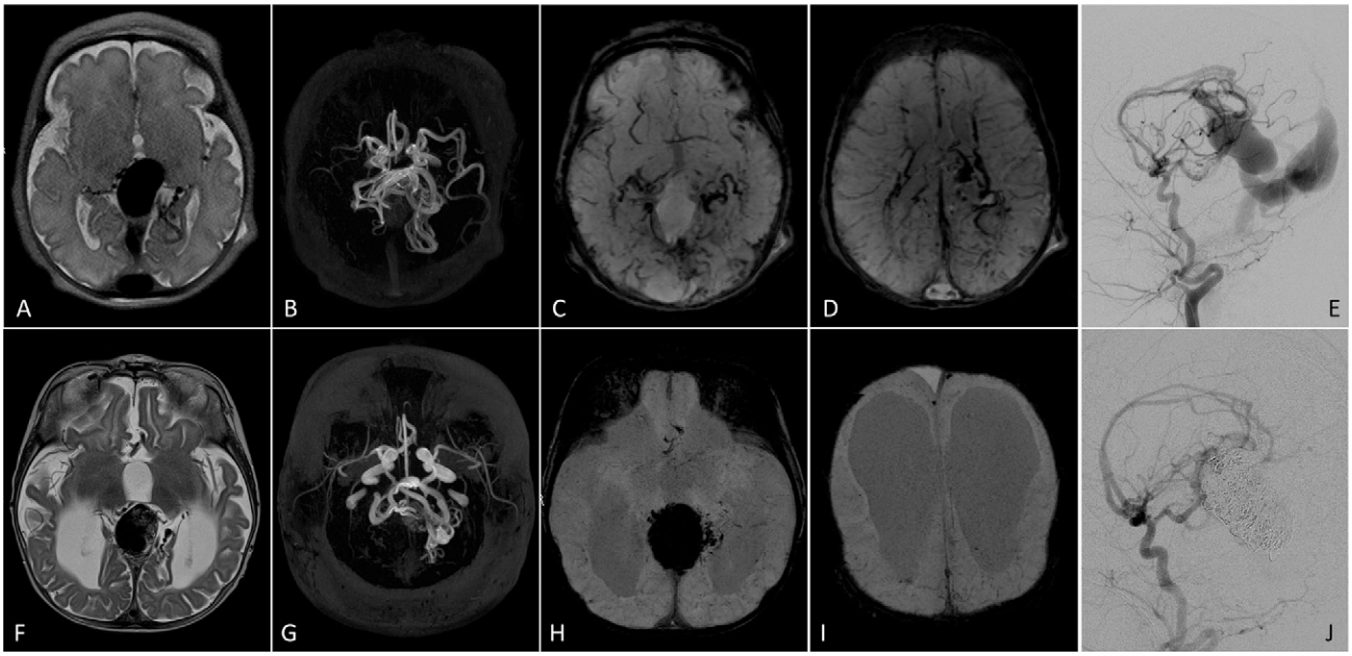

Fig. 1. Case no. 3.

other 2 children had a c̈oil massïn the vein of Galen. Subependymal and intramedullary were non-visible on SWI in 2 (out of 3) children, and remained SWI-hypointense, visible and dilated in 1 (out of 3) child (Case 5). Sulcal veins were non-visible on SWI in one child (Case 4) and remained SWI-hypointense, visible and dilated in 2 patients.

One child (Case 4) received 2 additional sessions of endovascular embolization, where a complete reduction of AV shunting in the VGAM was achieved; the latest was 141 days after the second follow-up MRI. A third follow-up MRI performed 84 days after the last embolization session revealed severe ventriculomegaly with mildly widened subarachnoid spaces, while subependymal, intramedullary and sulcal veins were non-visible. The vein of Galen was packed with a "coil mass".

All patients were discharged with no in-hospital mortality. Detailed postprocedural complications and clinical findings at discharge are listed in Table 3.

Correlation of SWI findings with angiographic and clinical outcome

Overall, normalization of the dilatation and hypointensity of cerebral veins on SWI was moderately correlated with the degree of the AV shunting reduction after staged embolization ($r = 0.41$, $P = 0.5$) and there was weak correlation with the degree of postprocedural hydrocephalus ($r = 0.19$, $P = 0.76$). The degree of cerebral vein SI normalization on SWI showed a negative correlation with postprocedural complications ($r = -0.41$, $P = 0.5$) and a moderate correlation with the clinical outcome ($r = 0.41$, $P = 0.5$).

Discussion

The currently accepted treatment for VGAM is staged endovascular embolization [1,7,8]. Due to contrast medium limitations and potential side effects of both Iodine- [23] and Gadolinium-based contrast media [24], a non-invasive, non-contrast based and radiation-free imaging modality would be beneficial for the evaluation of treatment response in this patient population. Recently, a report by Jagadeesan et al [17] has discussed the utility of SWI in differentiating between passive venous congestion and arterialized superficial veins in VGAM patients at a baseline study. SWI enables the evaluation of intraparenchymal venous hypertension/dilated intraparenchymal veins based upon the intrinsic SWI-hypointense signal of the veins. The degree of intraparenchymal venous prominence may serve as an indirect indicator of arteriovenous shunting in VGAM. In our study we observed 2 patterns of passive venous congestion in infants in response to staged embolization. The first pattern (Figs. 1 and 2) was associated with a mild to severe venous congestion status on SWI (including subependymal, intra-medullary and/or sulcal veins) at the baseline MRI study, which nearly completely resolved after the first staged endovascular embolization session (Case 1–4), irrespective of the degree of AV shunt reduction and with even moderately persistent AV shunting into the VGAM (Case 2 and 4). The second pattern (Fig. 3) was associated with extensive passive venous congestion on SWI, which showed no improvement after multiple sessions of endovascular treatment, including full embolization of the venous sac (Case 5). In the last case, the patient developed significant intraventricular hemorrhage after endovascular embolization of the venous sac of VGAM. The etiology of intraventricular hemorrhage and the fact that passive venous congestion persisted on SWI after the first session of endovascular embolization in this case remains unclear. Although, another patient (Case 4) developed a parafalcine intracranial hemorrhage (SDH, SAH and parenchymal hemorrhage) after the first staged embolization session with significant reduction of passive venous congestion on SWI, the etiology of such hemorrhage was most probably related to the chronic occlusion of the adjacent superior sagittal sinus in this case. Such a difference in the appearance of deep and superficial veins on SWI after staged embolization was not explained with the level of oxygen saturation (average SaO2 99.1% under GA and > 95% in natural sleep) or the type of anesthetic agent used in GA (Isoflurane in 9 MR studies and Sevoflurane in 1 MR study). Hydrocephalus as a clinical manifestation in VGAM is reported in up to 46.8% of cases in the literature, while the rate of hydrocephalus requiring shunting procedure was 17.9% [25]. In our cohort 40% of patients had moderate ventriculomegaly on baseline MR and 40% of patients required VP-shunt placement due to progressive hydrocephalus. There was however

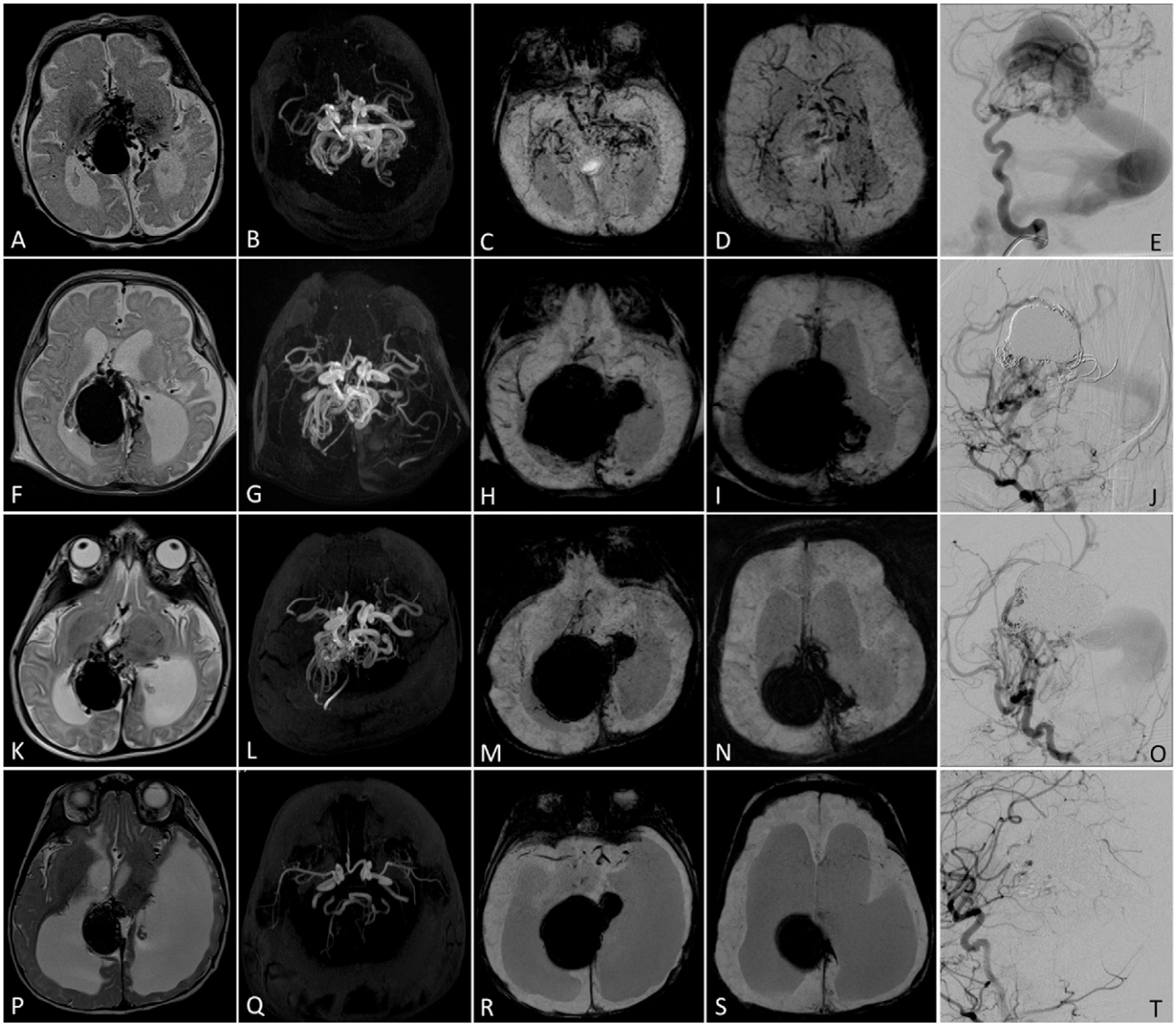

Fig. 2. Case no. 4.

Table 3
Imaging findings after staged embolization sessions and clinical outcome at discharge.

No.	Pre-procedural MRI			1st FU MRI		
	Ventriculomegaly	Subarachnoid spaces widened	Cerebral veins on SWI	Ventriculomegaly	Subarachnoid spaces wideness	Cerebral veins on SWI
1	Mild	Mild	Visible and dilated (Intra-medullary veins)*	No	No	Non visible
2	Moderate	No	Visible and dilated[a]	Moderate	Mild	Visible and dilated (Sulcal veins)
3	No	Mild	Visible and dilated[a]	Severe	Moderate	Non visible
4	Moderate	Mild	Visible and dilated[a]	Severe	Mild	Non visible
5	No	Mild	Visible and dilated[a]	Moderate	Mild	Visible and dilated
5	Moderate to severe intra-ventricular hemorrhage after complete occlusion of VGAM			Adequate physical and neurological development		

[a] Visible and dilated; refers to subependymal, intramedullary and sulcal veins, expect when otherwise specified.

no correlation between the progression of hydrocephalus and the status of venous congestion on SWI.

Previous reports [21,22] have shown the benefit of SWI in depicting cortical venous engorgement in adults with DAVF, which resolved after embolization of the DAVF in one case series [26]. In the pediatric population, Jagadeesan et al [17] showed that SWI was very accurate in differentiating between low and high-flow vascular anomalies of the vein of Galen. In our series, all patients had

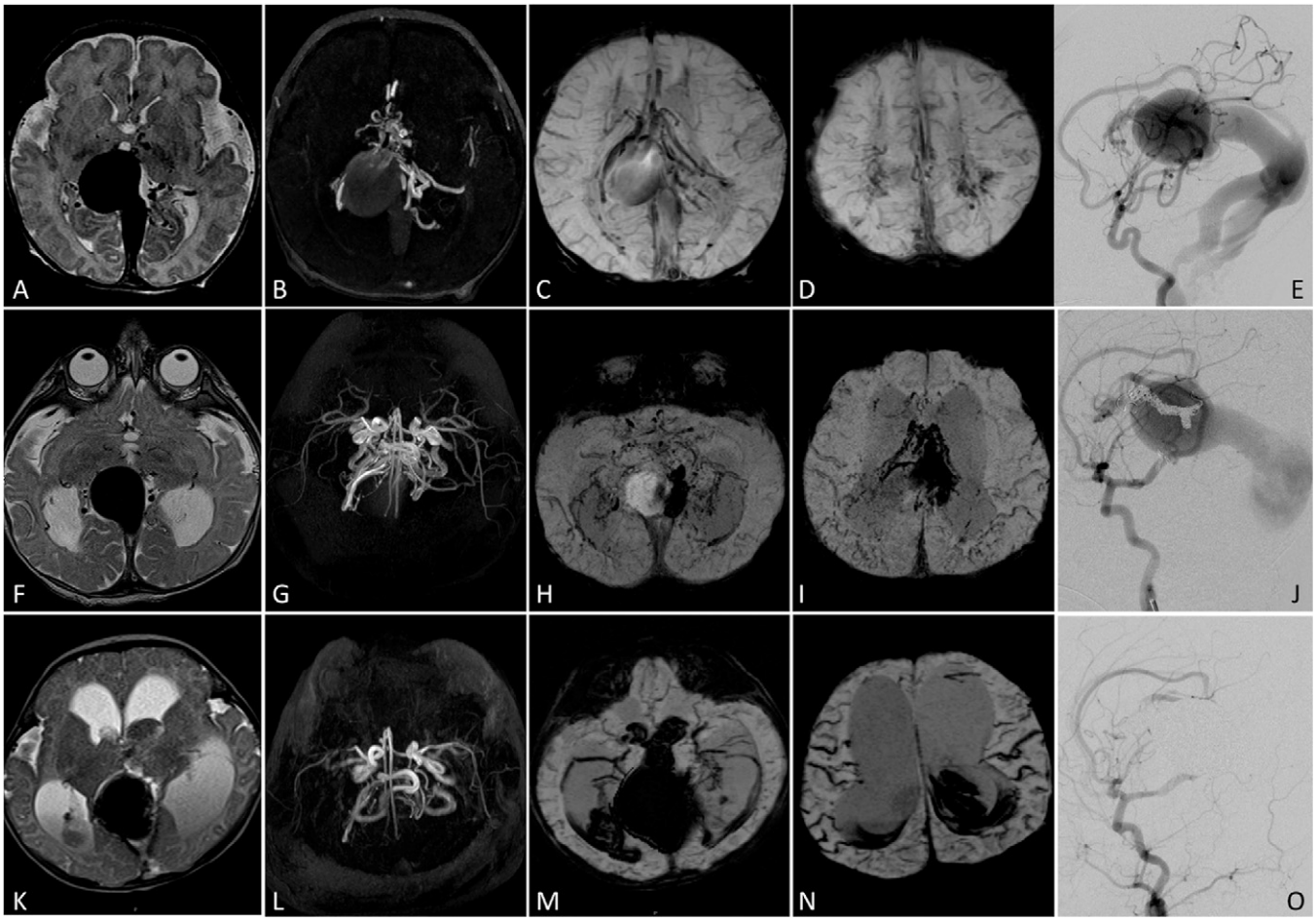

Fig. 3. Case no. 5.

VGAM of mural type, which is a high-flow lesion and so all presented with SWI-hyperintense signal of the vein of Galen on initial MR secondary to the high percentage of arterial oxygenated blood within the vein of Galen. This SWI-hyperintense signal persisted in the dilated vein of Galen after partial embolization (Fig. 3). The dilated subependymal, intramedullary and sulcal veins appeared SWI-hypointense in all children, due to passive venous congestion, where the delayed venous drainage allows for a relative decrease in oxygenated hemoglobin and increase in deoxygenated hemoglobin [21,27]. Interestingly enough, such a passive venous congestion state in VGAM did resolve to a great extent in 80% (4/5) of cases after only one session of endovascular treatment, with no correlation to the extent in reduction of the AV shunting as judged by DSA (mild reduction in 2 patients and significant in 2 patient). Such patterns of venous congestion and the changes depicted on SWI after treatment were not obvious on other sequences such as T2 weighted, TOF angiography (Fig. 1 and 2) or dynamic contrast enhanced MR venography, which emphasizes the importance of these SWI findings and its potential decision making role in the embolization in VGAM patients. While there was no clear correlation in our small cohort between normalization of cerebral vein appearance on SWI after initial stage of endovascular treatment and overall neurological complication rate or clinical outcome, we noticed a major neurological complication in the only case (case 5) of persistent cerebral venous congestion manifested as persistent hypointensity and dilatation of cerebral veins on SWI. The implications of persistent passive venous congestion after the initial endovascular embolization session remain to be determined though. While delaying the complete occlusion of the venous pouch of the VGAM has to be taken into consideration, in order to reduce the risk of intracranial hemorrhage, the accompanying heart failure and pulmonary hypertension, especially in neonates, requires an expedited significant reduction of AV shunting in order to control these symptoms. Future, larger scale studies may address this question.

Major limitations of our study are the retrospective nature of this analysis and the low number of cases available for review. Larger studies are needed to validate the described cerebral venous patterns as noted on SWI and their clinical significance.

Conclusion

To our knowledge, this is the first report to describe the utility of the SWI sequence in the evaluation of staged endovascular treatment of VGAM. Based on our preliminary findings, SWI seems to offer a non-invasive tool for evaluating passive cerebral venous congestion in pediatric patients with VGAM. The venous congestion remained undetected on conventional T1 and T2-weighted MRI as well as MR-angiography/venography. The novel finding in our study points toward a noticeable reduction in passive venous congestion in 80% of pediatric cases with VGAM, even after one session of staged endovascular embolization. This change of venous congestion status did not appear to correlate with the estimated amount of reduction in AV shunting after embolization on DSA or the degree of hydrocephalus. Further studies are needed to assess these findings in this rare vascular disorder.

Case 3

Neonate with prenatally diagnosed VGAM, who presented at birth with cardiomegaly and poor cardiac function. MRI was done at day 1 of life (A–D) to evaluate the malformation; ***A***. T2 weighted image shows the dilated vein of Galen with normal size of the ventricular system, no parenchymal edema is noted; B. Time of flight (TOF) MR angiography shows the dilated vessels of circle of Willis and AV shunting into the vein of Galen; C–D. minIP SWI images show a hyperintense signal of the arterialized blood in the vein of Galen due to AV shunting and a SWI-hypointense signal of the visible and dilated subependymal, intramedullary and sulcal veins bilaterally as a sign of passive venous congestion; E. DSA, right common carotid artery injection, lateral view shows the prominent and dilated posterior and anterior choroidal arteries feeding the VGAM of mural type.

J. DSA, right common carotid artery injection, lateral view, interval staged endovascular embolization of the feeding arteries as well as the venous sac was performed with near complete reduction in AV shunting.

Follow-up MRI (F-I) performed at 7.7 months of age; F. T2 weighted image shows the T2-hypointense "coil mass" in the vein of Galen, which has decreased in size, and interval development of severe hydrocephalus; G. TOF angiography shows persistent dilated vessels of circle of Willis without shunting into the now coiled vein of Galen; H-I. SWI sequence with interval coil mass induced magnetic susceptibility related signal void within the vein of Galen and significant reduction of the venous congestion manifested as non-visualized subependymal, intramedullary and sulcal veins.

Case 4

A female neonate with VGAM presented shortly after birth with congestive heart failure and pulmonary hypertension. MRI at 11-days of age (A–D); A. T2 weighted image shows the dilated vein of Galen with moderate enlargement of the ventricular system; B. TOF angiography shows the dilated vessels of circle of Willis and AV shunting into the vein of Galen; C–D. SWI sequence shows the hypointense signal of the visible and dilated subependymal, intramedullary and sulcal veins bilaterally. The dilated vein of Galen shows a SWI-hyperintense signal secondary to the highly oxygenated blood within the vein as result of the AV shunting.

E. DSA, right internal carotid artery injection, lateral view the VGAM of mural type prior to embolization. J. DSA, left internal carotid artery injection, lateral view, first session of staged endovascular embolization of the feeding arteries and venous sac with mild reduction in AV shunting at age of 15 days.

Follow-up MRI (F–I) at 1 month of age; F. T2 image showing the T2-hypointense "coil mass" in the vein of Galen, and interval development of severe hydrocephalus; ***G***. TOF angiography shows persistent dilated vessels of circle of Willis; H–I. SWI images with interval "coil mass" induced magnetic susceptibility related signal void of the vein of Galen and significant reduction in the intraparenchymal and subependymal venous congestion. The patient developed an interval left parafalcine SDH, SAH and frontoparietal parenchymal hemorrhage (not shown).

O. DSA, right common carotid artery injection, lateral view, after 2 session of staged endovascular embolization with mild reduction of AV shunting at 1.6 months of age.

Follow-up MRI (K–N) at 3 months of age; K. T2 image showing persistence of severe hydrocephalus; L. TOF angiography shows a reduction of dilated vessels of circle of Willis; M–N. SWI images with unchanged significant reduction in the venous congestion.

T. DSA, right common carotid artery injection, lateral view, after 2 session of staged endovascular embolization with complete reduction of AV shunting at 7.5 months of age.

Follow-up MRI (P–S) at 10.5 months of age; P. T2 image showing progressive severe hydrocephalus, decrease in size of the vein of Galen and interval significant post-hemorrhagic brain parenchymal loss in the left hemisphere; Q. TOF angiography shows normalization of the caliber of circle of Willis; R–S. SWI images showing no sign of venous congestion.

Case 5

Male neonate with prenatally diagnosed VGAM, who presented after birth with seizures, pulmonary hypertension, heart failure and macrocephaly.

MRI at age of 6 days (A–D) was done to evaluate the malformation; A. T2 weighted image shows the dilated vein of Galen with a normal size of the ventricular system, there is no parenchymal edema appreciated; B. Sagittal TOF MR angiography/venography shows the high-flow AV shunting into the arterialized vein of Galen, straight sinus as well as transverse/sigmoid sinuses; C–D. SWI sequence shows the SWI-hyperintense signal of the vein of Galen due to AV shunting and a hypointense signal of the visible and dilated subependymal, intramedullary and sulcal veins bilaterally, representing venous congestion; E. DSA, left internal carotid artery injection, lateral view showing the prominent and dilated posterior and anterior choroidal arteries feeding the VGAM. J. DSA, right internal carotid artery injection, lateral view; interval staged endovascular embolization of the feeding arteries with mild reduction (< 33%) of AV shunting.

First follow-up MRI (F–I) performed at 3.2 months of age; F. T2 weighted MR image shows a relative decrease in size of vein of Galen with interval development of moderate hydrocephalus; G. Axial TOF MR angiography shows persistent dilated arterial feeders as well as AV shunting into VGAM; ***H-I***. SWI sequence with persistent passive venous congestion, with SWI-hypointense subependymal, intramedullary and sulcal veins which are still visible and dilated.

O. DSA, right common carotid artery injection, lateral view; subsequent staged endovascular treatment with embolization of the venous sac was performed with near complete reduction in AV shunting (> 66%).

Second follow-up MRI (K–N) performed at 3.9 months of age after coil embolization of the venous sac, the patient presented with an interval moderate to severe intraventricular hemorrhage; K. T2 weighted MR image with "coil mass" in the vein of Galen, worsening of hydrocephalus and interval intraventricular hemorrhage; L. TOF MR angiography shows a normal arterial vasculature with no evidence of AV shunting into VGAM; M–N. SWI sequence with persistent SWI-hypointense signal of the visible and dilated subependymal, intramedullary and sulcal veins, representing venous congestion even after embolization of the venous sac, interval appearance of intraventricular hemorrhage induced susceptibility artifacts.

Case 1

Female infant with a prenatally diagnosed VGAM, who presented 2 weeks after birth with mild right ventricular hypertrophy. MRI done at 4 months of age; A. T2 weighted image shows a mildly dilated vein of Galen with mild ventricular enlargement; B. TOF MRA shows the dilated vessels of circle of Willis and AV shunting into the vein of Galen pouch; C–D. minIP SWI images show a hyperintense signal of the vein of Galen and a hypointense signal of the visible and dilated intramedullary veins; E. DSA, right common carotid artery injection, lateral view, at the same day shows the mildly dilated anterior choroidal arteries feeding the VGAM of mural type.

J. DSA, right common carotid artery injection, lateral view, after a single session of endovascular embolization of the feeding arteries (same day as E) with a significant reduction in arteriovenous shunting.

Follow-up MRI (F–I) performed at 12 months of age; F. T2 weighted image shows a normalization of both the vein of Galen and ventricular system width; G. TOF angiography shows persistent dilated vessels of circle of Willis without shunting into the now coiled vein of Galen; H–I. minIP SWI images showing coil related signal void lateral to the vein of Galen on the right, disappearance of the SI hyperintensity in the vein of Galen and complete regression of the formerly prominent intramedullary veins.

Case 2

Male neonate who presented at birth with persistent pulmonary hypertension of newborn and cardiomegaly. MRI done at day 7 of life; A. T2 weighted image shows a significantly dilated vein of Galen with moderate ventricular enlargement; B. TOF MRA shows dilated posterior choroidal feeders and AV shunting into the vein of Galen pouch; C–D. minIP SWI images show a hyperintense signal of the vein of Galen and a hypointense signal of the visible and dilated cortical, subependymal and intramedullary veins; E. DSA, left common carotid artery injection, lateral view, at 4 months of life shows large dilated posterior choroidal arteries bilaterally feeding the significantly dilated venous pouch of the VGAM of mural type.

J. DSA, left common carotid artery injection, lateral view, after the first session of endovascular embolization of two right posterior medial choroidal branches (same day as ***E***) with a mild reduction in arteriovenous shunting.

Follow-up MRI (F–I) performed at 8 months of age; F. T2 weighted image shows an increase in the size of the vein of Galen and persistence of the moderately dilated ventricular system. Note the void artifact in the temporo-occpiptal region on the right side (F–I) due to a newly placed ventriculoperitoneal shunt with the tip in the right lateral ventricle to manage the hydrocephalus; G. TOF angiography shows persistent dilated choroidal arteries shunting into the vein of Galen; H–I. minIP SWI images showing coil related signal void lateral to the vein of Galen bilaterally, persistence of the SI hyperintensity in the vein of Galen and resolution of the prominent intramedullary and subependymal veins with residual dilated and hypointense cortical veins bilaterally.

O. DSA, right common carotid artery injection, lateral view, at 9 months of age after two more session of endovascular embolization of the residual feeding arteries with a complete occlusion of the arteriovenous shunting to the vein of Galen.

Follow-up MRI (K–N) performed at 9 months of age (same day as O); K. T2 weighted image shows persistence of the venous pouch and reduction of the currently mildly dilated ventricular system width; L. TOF angiography shows absence of flow signal into the vein of Galen; M–N. minIP SWI images show persistence of the SI hyperintensity in the vein of Galen and residual minimally dilated cortical veins bilaterally with complete resolution of the subependymal and intra-medullary veins.

Disclosure of interest

The authors declare that they have no competing interest.

Appendix A. Supplementary data

Supplementary material related to this article can be found, in the online version, at https://doi.org/10.1016/j.neurad.2018.09.009.

References

[1] Casasco A, Lylyk P, Hodes JE, et al. Percutaneous transvenous catheterization and embolization of vein of galen aneurysms. Neurosurgery 1991;28:260–6.
[2] Lasjaunias P, Terbrugge K, Piske R, et al. [Dilatation of the vein of Galen. Anatomoclinical forms and endovascular treatment apropos of 14 cases explored and/or treated between 1983 and 1986]. Neurochirurgie 1987;33:315–33.
[3] J. M. Entwicklung der Sinus durae matris und der Hirnvenen des Menschen. Bulletin International de l'Academie des Sciences et des Lettres 1921; Classe des Sciences Mathematiques et Naturelles.
[4] Lasjaunias P, Garcia-Monaco R, Rodesch G, et al. Deep venous drainage in great cerebral vein (vein of Galen) absence and malformations. Neuroradiology 1991;33:234–8.
[5] Berenstein A, Toma N, Niimi Y, et al. Occlusion of posterior fossa dural sinuses in vein of Galen malformation. AJNR Am J Neuroradiol 2016;37:1092–8.
[6] Frawley GP, Dargaville PA, Mitchell PJ, et al. Clinical course and medical management of neonates with severe cardiac failure related to vein of Galen malformation. Arch Dis Child Fetal Neonatal Ed 2002;87:F144–149.
[7] Lasjaunias PL, Chng SM, Sachet M, et al. The management of vein of Galen aneurysmal malformations. Neurosurgery 2006;59:S184–94 [discussion S183–S113].
[8] Yan J, Wen J, Gopaul R, et al. Outcome and complications of endovascular embolization for vein of Galen malformations: a systematic review and meta-analysis. J Neurosurg 2015;123:872–90.
[9] Gailloud P, O'riordan DP, Burger I, et al. Confirmation of communication between deep venous drainage and the vein of galen after treatment of a vein of Galen aneurysmal malformation in an infant presenting with severe pulmonary hypertension. AJNR Am J Neuroradiol 2006;27:317–20.
[10] Pearl M, Gomez J, Gregg L, et al. Endovascular management of vein of Galen aneurysmal malformations. Influence of the normal venous drainage on the choice of a treatment strategy. Childs Nerv Syst 2010;26:1367–79.
[11] Alvarez H, Garcia Monaco R, Rodesch G, et al. Vein of galen aneurysmal malformations. Neuroimaging Clin N Am 2007;17:189–206.
[12] Gailloud P, O'Riordan DP, Burger I, et al. Diagnosis and management of vein of galen aneurysmal malformations. J Perinatol 2005;25:542–51.
[13] Steggerda SJ, Leijser LM, Wiggers-de Bruïne FT, et al. Cerebellar injury in preterm infants: incidence and findings on US and MR images. Radiology 2009;252:190–9.
[14] Kutanzi KR, Lumen A, Koturbash I, et al. Pediatric exposures to ionizing radiation: carcinogenic considerations. Int J Environ Res Public Health 2016;13.
[15] Meoded A, Poretti A, Northington FJ, et al. Susceptibility weighted imaging of the neonatal brain. Clin Radiol 2012;67:793–801.
[16] Verschuuren S, Poretti A, Buerki S, et al. Susceptibility-weighted imaging of the pediatric brain. AJR Am J Roentgenol 2012;198:W440–9.
[17] Jagadeesan BD, Cross DT, Delgado Almandoz JE, et al. Susceptibility-weighted imaging: a new tool in the diagnosis and evaluation of abnormalities of the vein of Galen in children. AJNR Am J Neuroradiol 2012;33:1747–51.
[18] Haacke EM, Mittal S, Wu Z, et al. Susceptibility-weighted imaging: technical aspects and clinical applications, part 1. AJNR Am J Neuroradiol 2009;30:19–30.
[19] Hodel J, Rodallec M, Gerber S, et al. Susceptibility weighted magnetic resonance sequences "SWAN, SWI and VenoBOLD": technical aspects and clinical applications. J Neuroradiol 2012;39:71–86.
[20] Hiremath SB, Anantrao Gautam A, Anil S, et al. Susceptibility-weighted angiography and diffusion-weighted imaging in posterior reversible encephalopathy syndrome - Is there an association between hemorrhage, cytotoxic edema, blood pressure and imaging severity? J Neuroradiol 2017;44:319–25.
[21] Saini J, Thomas B, Bodhey NK, et al. Susceptibility-weighted imaging in cranial dural arteriovenous fistulas. AJNR Am J Neuroradiol 2009;30:E6.
[22] Noguchi K, Kuwayama N, Kubo M, et al. Intracranial dural arteriovenous fistula with retrograde cortical venous drainage: use of susceptibility-weighted imaging in combination with dynamic susceptibility contrast imaging. AJNR Am J Neuroradiol 2010;31:1903–10.
[23] Schooler GR, Zurakowski D, Lee EY. Evaluation of contrast injection site effectiveness: thoracic CT angiography in children with hand injection of IV contrast material. AJR Am J Roentgenol 2015;204:423–7.
[24] Neeley C, Moritz M, Brown JJ, et al. Acute side effects of three commonly used gadolinium contrast agents in the paediatric population. Br J Radiol 2016;89:20160027.
[25] Zerah M, Garcia-Monaco R, Rodesch G, et al. Hydrodynamics in vein of Galen malformations. Childs Nerv Syst 1992;8:111–7 [discussion 117].
[26] Nakagawa I, Taoka T, Wada T, et al. The use of susceptibility-weighted imaging as an indicator of retrograde leptomeningeal venous drainage and venous congestion with dural arteriovenous fistula: diagnosis and follow-up after treatment. Neurosurgery 2013;72:47–54 [discussion 55].
[27] Polan RM, Poretti A, Huisman TA, et al. Susceptibility-weighted imaging in pediatric arterial ischemic stroke: a valuable alternative for the non-invasive evaluation of altered cerebral hemodynamics. AJNR Am J Neuroradiol 2015;36:783–8.